Allerhand, A. (1978) *Acc. Chem. Res. 11*, 469.
Allerhand, A., & Komoroski, R. A. (1973) *J. Am. Chem. Soc. 95*, 8228.
Allerhand, A., Doddrell, D., & Komoroski, R. A. (1971) *J. Chem. Phys. 55*, 189.
Bothner-By, A. A., & Johner, P. E. (1978) *Biophys. J. 24*, 779.
Bull, T. E., Norne, J. E., Reimarsson, P., & Lindman, B. (1978) *J. Am. Chem. Soc. 100*, 4643.
Canet, D., Nery, H., & Brondeau, J. (1979) *J. Chem. Phys. 70*, 2098.
Deslauriers, R., & Smith, I. C. P. (1977) *Biopolymers 16*, 1245.
Dill, K., & Allerhand, A. (1979) *J. Am. Chem. Soc. 101*, 4376.
Gupta, R. K. (1977) *J. Magn. Reson. 25*, 231.
Gutowsky, H. S., McCall, D. W., & Slichter, C. P. (1953) *J. Chem. Phys. 21*, 279.
Howarth, O. W. (1979) *J. Chem. Soc., Faraday Trans. 2 75*, 863.
Jeffers, P. K., Sutherland, W. M., & Khalifah, R. G. (1978) *Biochemistry 17*, 1305.
Komoroski, R. A., Peat, I. R., & Levy, G. C. (1975) *Biochem. Biophys. Res. Commun. 65*, 272.
Lange, N. A. (1961) *Handbook of Chemistry*, McGraw-Hill, New York.
London, R. E. (1980) in *Magnetic Resonance in Biology* (Cohen, J. S., Ed.) p 1–69, Wiley-Interscience, New York.
London, R. E., & Avitabile, J. (1976) *J. Chem. Phys. 65*, 2443.
London, R. E., Matwiyoff, N. A., Kollman, V. H., & Mueller, D. D. (1975a) *J. Magn. Reson. 18*, 555.
London, R. E., Matwiyoff, N. A., & Mueller, D. D. (1975b) *J. Chem. Phys. 63*, 4442.
London, R. E., Stewart, J. M., Williams, R., Cann, J. R., & Matwiyoff, N. A. (1979) *J. Am. Chem. Soc. 101*, 2455.
Moreland, C. G., & Carroll, F. E. (1974) *J. Magn. Reson. 15*, 596.
Nery, H., & Canet, D. (1981) *J. Magn. Reson. 42*, 370.
Norton, R. S., & Allerhand, A. (1976) *J. Am. Chem. Soc. 98*, 1007.
Pople, J. A. (1958) *Mol. Phys. 1*, 168.
Richarz, R., Nagayama, K., & Wuthrich, K. (1980) *Biochemistry 19*, 5189.
Schaublin, S., Hohener, H., & Ernst, R. R. (1974) *J. Magn. Reson. 13*, 196.
Shimizu, H. (1964) *J. Chem. Phys. 40*, 3357.
Suzuki, K. T., Cary, L. W., & Kuhlmann, K. F. (1975) *J. Magn. Reson. 18*, 390.
Virlet, J., & Ghesquieres, D. (1980) *Chem. Phys. Lett. 73*, 323.
Wang, C. C., & Pecora, R. (1980) *J. Chem. Phys. 72*, 5333.

The Protein Synthesis Inhibitor Thermorubin. 1. Nature of the Thermorubin–Ribosome Complex†

Fwu-lai Lin‡ and Arnold Wishnia*

ABSTRACT: Thermorubin behaves as a triprotic acid, TrH_3, with pK_as of 4.7, 7.1, and 9.1 (22 °C, 10% v/v aqueous ethanol, corrected to zero ionic strength). Mg^{2+} successively forms TrH·Mg and $Tr{\cdot}Mg_2^+$ complexes with formation constants $L_{11} = [TrH{\cdot}Mg]/([Mg^{2+}][TrH^{2-}]) = 3.3 \times 10^4\ M^{-1}$ and $L_{12H} = [Tr{\cdot}Mg_2^+][H^+]/([TrH{\cdot}Mg][Mg^{2+}]) = 1.4 \times 10^{-5}$. The first proposed structure (I) [Moppett, E., Dix, D. T., Johnson, F., & Coronelli, C. (1972) *J. Am. Chem. Soc. 94*, 3269–3272] is incompatible with these results. The pK_a's of TrH_3 are compatible with ionization of the carboxylic acid, the enolic β-diketone, and one of the phenolic groups of the new structure (II) [Johnson, F., Chandra, B., Iden, C. R., Naiksatam, P., Kahen, R., Okaya, Y., & Lin, S.-Y. (1980) *J. Am. Chem. Soc. 102*, 5580–5585]. Plausible structures for TrH·Mg and $Tr{\cdot}Mg_2^+$ can be suggested. All species have absorbance maxima near 300, 330, and 430 nm, with absorptivities of 30–60, 20–50, and 15–20 $mM^{-1}\ cm^{-1}$, respectively. TrH_n and TrH·Mg have broad featureless emission spectra, maximal at 585 nm, with quantum yields of about 0.004 and 0.010. $Tr{\cdot}Mg_2^+$ is not fluorescent. TrH·Mg and $Tr{\cdot}Mg_2^+$ are the predominant species at intracellular ionic concentrations. Centrifuge and fluorescence enhancement studies show that *Escherichia coli* 70S ribosomes and 30S and 50S subunits all have a single site for binding thermorubin, with $K_D = 1.9 \times 10^{-8}$, 1.9×10^{-6}, and 1.4×10^{-6} M (25 °C, 10 mM Mg^{2+}, 60 mM M^+, pH 7.5). Thermorubin binds to ribosomes more strongly than streptomycin and binds orders of magnitude more strongly than the structurally comparable tetracyclines. The limiting fluorescence enhancements, $E_\infty = (F_{bound,molar}/F_{free,molar}) - 1$, are 0.54, 1.41, and 1.53 (for 70 S, 30 S, and 50 S, respectively). Iodide ion quenching of free Tr, 30 S·Tr, and 50 S·Tr follows the same Stern–Volmer curve, while 70 S·Tr fluorescence is not quenched at all: the thermorubin binding sites must lie on the surfaces of the 30S and 50S subunits and inside the 70S particles. It is not improbable that the weaker subunit sites are corresponding portions of the strong 70S site. It is very likely that the actual inhibitory species is the neutral fluorescent TrH·Mg complex.

The antibiotic thermorubin, discovered in 1964 (Craveri et al., 1964), was later shown to inhibit protein synthesis, but not DNA and RNA synthesis, in *Escherichia coli* in vivo and to inhibit initiator tRNA binding to ribosomes in vitro (Pirali et al., 1974). Our concern in this paper is the identity of the effective species among the set at equilibrium in physiological ionic solutions and the elementary characterization of its target: the number, location, and affinity of the principal ribosomal binding site(s). The unusual, perhaps unique, mode of action of thermorubin is described in the following paper (Lin & Wishnia, 1982).

† From the Department of Chemistry, State University of New York at Stony Brook, Stony Brook, New York 11794. *Received June 5, 1981; revised manuscript received September 21, 1981.* Taken, in part, from the thesis of F.-l.L., submitted in partial fulfillment of the requirements for Ph.D., State University of New York at Stony Brook. Supported in part by National Institutes of Health Grant GM27176.

‡ Present address: Cancer Biology Program, Frederick Cancer Research Center, National Cancer Institute, Frederick, MD 21701.

0006-2960/82/0421-0477$01.25/0

The structure I, proposed in 1972 (Moppett et al., 1972), could be expected to have useful fluorescence properties, as well as H^+ and M^{2+} equilibria that required characterization.

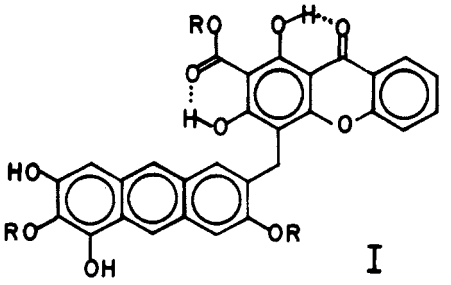

I

However, it became immediately apparent that structure I was incompatible with the results we report here, an observation which spurred efforts already in course to obtain a crystallographic structure for thermorubin (II) (Johnson et al., 1980)

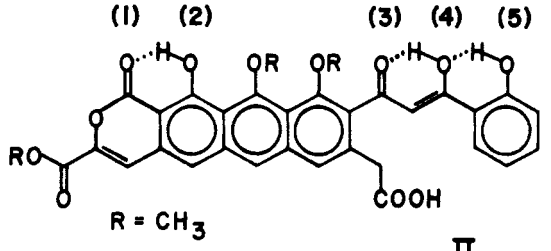

II

Structure II has affinities with the four fused ring structure of tetracycline, and both bind divalent cations. Conceivably, their biosynthesis may have similar features. However, tetracycline binds to *E. coli* ribosomes in a somewhat bizarre multiple binding site pattern, with small formation constants [Fey et al., 1973; White & Cantor, 1971; cf. Tritton (1977)]. The binding of thermorubin to ribosomes is quite simple: the 70S particle possesses a high-affinity site for binding a single molecule of thermorubin, and single, weaker sites are found on both the 30S and 50S ribosomal subunits.

Materials and Methods

Thermorubin. The compound generously supplied by Professor Francis Johnson had been shown to give only one component in thin-layer and high-pressure liquid chromatography [cf. Johnson et al. (1980)]. It behaved as a single component in our ribosome binding studies, unlike aurintricarboxylic acid which fractionated into spectroscopically distinct high and low ribosome affinity populations. Tr obeys Beer's law across the spectrum, indicating that all Tr species remain monomeric, up to the aqueous solubility limit.

Thermorubin is stable indefinitely in cold $CHCl_3$ in the dark and is not altered by 1–2-h manipulation in dilute aqueous solution at ambient or Cary 118 spectrophotometer light levels. Both reversible photoisomerization and irreversible decomposition can be produced in the Perkin-Elmer MPF-44A spectrophotofluorometer unless care is taken to minimize the actinic dosage. Thermorubin dissolved in dimethylformamide, dimethyl sulfoxide, and ethanol exhibits measurable decomposition on a time scale of hours. In general, the integrity of the compound must be verified spectrophotometrically after any series of experiments.

Thermorubin concentrations in solution are ultimately referred to a spectrophotometric titration with uranyl acetate at pH 7, in which the quantitative formation of the very stable $UO_2{\cdot}(TrH)_2^{2-}$ is monitored at 298 nm. This avoided the twin problems of the incorrect structure (I) and variable $CHCl_3$ content in the crystalline samples.

Ribosomes and 30S and 50S subunits were isolated from fresh or frozen MRE600 strain *E. coli* by standard procedures [cf. Wishnia & Boussert (1977) and Wishnia et al. (1975)]. All preparations showed the $[Mg^{2+}]$ dependence of the 30S + 50S = 70S equilibrium expected of "tight", type A species, with a midpoint near 2 mM Mg^{2+}, by light scattering or sucrose density gradient ultracentrifugation. In appropriate combinations, they were highly active in fMet-tRNA binding and poly(U)-dependent polyphenylalanine synthesis (Lin & Wishnia, 1982). The subunit preparations contained less than 2% cross-contamination as judged by the poly(Phe) synthesis assay. Ribosome concentrations were determined from the 260-nm absorbance (1 mg/mL gives A_{260} = 16, molecular weight 2.55×10^6).

Other Materials. The other compounds used in this work were of standard commercial analytical reagent purity. Approximately 1 M solutions of $Mg(OAc)_2$, $MgCl_2$, $CaCl_2$, $SrCl_2$, and $BaCl_2$ were standardized by displacement and subsequent titration of H^+ from a cation-exchange resin, and by Mohr method assays for Cl^-. Standard buffer for ribosomes is 60 mM NH_4Cl, 10 mM tris(hydroxymethyl)aminomethane, 10.5 mM (or variable) $MgCl_2$, 0.5 mM EDTA, and 7 mM 2-mercaptoethanol, pH 7.5, 22 °C.

H^+ and M^{2+} Equilibria of Thermorubin. Spectra spanning the desired range of pH (2–12) or $[M^{2+}]$ were recorded in 5-cm path-length cells for $\sim 10^{-6}$ M thermorubin in Chelex-100-pretreated 10% v/v ethanol–water, 5 mM acetate, imidazole, and/or tris(hydroxymethyl)aminomethane at 22 °C. pH control was ±0.001 unit. The sets of spectra were analyzed by using a multiwavelength nonlinear least-squares algorithm developed for the multiple iodomercurate–β-lactoglobulin equilibria (Stone & Wishnia, 1978). Minor formation of $Mg(OAc)^+$ was corrected for by using its formation constant of 17.6 M^{-1} at 25 °C (Nancollas, 1956). The actual sets of spectra, the computer program, and experimental details are available in Lin's thesis (Lin, 1978).

Thermorubin Binding to Ribosomes. For establishment of the stoichiometry, thermorubin and ribosomes, in outgassed standard buffer, 2% v/v dimethyl sulfoxide, were centrifuged overnight in polycarbonate tubes in a Spinco L5-50 preparative ultracentrifuge. The pellets were taken up in standard buffer without 2-mercaptoethanol and centrifuged briefly to remove macroscopic particles; their thermorubin content was determined either from the absorbance at 340 nm (corrected for the ribosome turbidity) or from the fluorescence at 550 nm (corrected for the trivial ribosome contribution). Recovery tests validated these procedures. The key fluorescence enhancement determinations of thermorubin binding are dealt with below.

Results and Discussion

(A) Thermorubin H^+–M^{2+} Equilibria. The presence of an isosbestic point in a set of spectra means that the transformations occurring among absorbing species, however complex, can be described by a single progress variable and a set of constants. The spectra of thermorubin between pH 2.3 and 12.0 present three pH regions, covering nearly the entire inverval, with well-marked sets of isosbestic points (cf. Figure 1): 344 nm, pH 2.3–5.5; 299 and 324 nm, pH 6.2–8.0; 299 and 352 nm, pH >8.5. The spectrum is virtually unchanged between pH 10.4 and 12.0, indicating that no acidic group is dissociating in this interval (the spectra are fully reversible between pH 2.3 and 10.4, but solutions exposed to pH 12 for

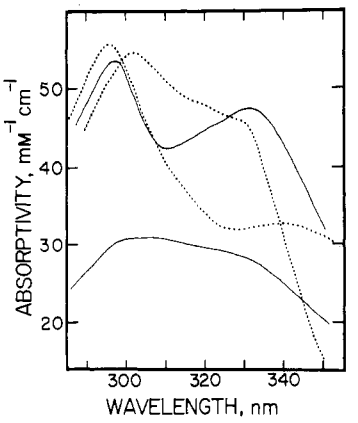

FIGURE 1: Spectra of $TrH_n^{(3-n)}$ species. Reading down at 320 nm, one observes the following species: TrH_2^- (···); TrH^{2-} (—); Tr^{3-} (···); TrH_3 (—). Curves calculated from fitting 70 spectra spanning pH 2.3–12.0, at ~2 × 10^{-6} M Tr. These curves reproduce the 70 experimental spectra with a standard deviation of 0.4% per point.

10–20 min do not fully recover their lower pH spectra). Such data can accommodate only three ionization equilibria:

$$TrH_3 \underset{+\,H^+}{\overset{K_1}{\rightleftharpoons}} TrH_2^- \underset{+\,H^+}{\overset{K_2}{\rightleftharpoons}} TrH^{2-} \underset{+\,H^+}{\overset{K_3}{\rightleftharpoons}} Tr^{3-} \qquad (1)$$

The computer fitting of these data yields spectra of the four species (Figure 1) and the values of the progressive thermodynamic dissociation constants: $K_1 = (2.1 \pm 0.1) \times 10^{-5}$ M ($pK_1 = 4.7$); $K_2 = (8.2 \pm 0.6) \times 10^{-8}$ M ($pK_2 = 7.1$); $K_3 = (8.1 \pm 0.7) \times 10^{-10}$ M ($pK_3 = 9.1$). As anticipated, such values can be attributed to a carboxylic acid, a β-diketone, and a phenolic hydroxyl group. While structure II of thermorubin contains four potentially ionizable protons, pK_4 for the remaining phenolic hydroxyl is, and of right ought to be, well above 12 (see part C of Results and Discussion).

Metal Ions. An apparent cumulative formation constant β_2 for the reaction

$$UO_2^{2+} + 2TrH^{2-} \rightleftharpoons UO_2{\cdot}(TrH)_2^{2-} \qquad (2)$$

can be extracted from the uranyl ion spectrophotometric titration of thermorubin, because a slight incompleteness (curvature) near the ML_2 equivalence point permits estimates of the concentrations of the species in eq 2 in this neighborhood. The value of β_2 at pH 7.0 is 1.2 × 10^{14} M^{-2}. Uranyl forms ML_2 complexes with almost all ligands; β_2 for the β-diketone acetylacetone, in water, is 2 × 10^{14} M^{-2} (Sillén & Martell, 1964).

The equilibria between thermorubin and Mg^{2+}, Ca^{2+}, Sr^{2+}, and Ba^{2+} were studied in detail at pH 7.50, where TrH^{2-} is the major metal-free species (75%). For the reasons examined in the Appendix (see paragraph at end of paper regarding supplementary material), we concluded that an ML_2 complex was not a significant species, in contrast to the case of $UO_2{\cdot}(TrH)_2^{2-}$, and that the observed spectra reflected the following reaction sequence:

$$TrH^{2-} + Mg^{2+} \rightleftharpoons TrH{\cdot}Mg$$

$$L_{11} = [TrH{\cdot}Mg]/([TrH^{2-}][Mg^{2+}]) \qquad (3.1)$$

$$TrH{\cdot}Mg \rightleftharpoons Tr{\cdot}Mg^- + H^+$$

$$K_{3M} = [Tr{\cdot}Mg^-][H^+]/[TrH{\cdot}Mg] \qquad (3.2)$$

$$Tr{\cdot}Mg^- + Mg^{2+} \rightleftharpoons Tr{\cdot}Mg_2^+$$

$$L_{12} = [Tr{\cdot}Mg_2^+]/([Tr{\cdot}Mg^-][Mg^{2+}]) \qquad (3.3)$$

$$TrH{\cdot}Mg + Mg^{2+} \rightleftharpoons Tr{\cdot}Mg_2^+ + H^+$$

$$L_{12H} = [Tr{\cdot}Mg_2^+][H^+]/([TrH{\cdot}Mg][Mg^{2+}]) \qquad (3.4)$$

Table I: Formation Constants of Thermorubin·M^{2+} Complexes[a]

ion	$L'_{11} \times 10^{-3}$ (M^{-1})	$L'_{12} \times 10^{-2}$ (M^{-1})	$L_{11} \times 10^{-3}$ (M^{-1})	L_{12H}[b] × 10^6
Mg^{2+}	32.7 ± 1.9	3.98 ± 0.39	32.5 ± 2.0	13.7 ± 1.7
Ca^{2+}	9.6 ± 1.2	1.51 ± 0.22	10.3 ± 1.4	6.8 ± 1.2
Sr^{2+}	2.0 ± 0.2	0.19 ± 0.05	2.5 ± 0.2 (2.6–3.1)	0.7 ± 0.1 (0.8–1.4)
Ba^{2+}	4.3 ± 1.0 (1.5)	0.42 ± 0.06 (0.18)	5.6 ± 1.4 (4.0–5.6)	1.5 ± 0.3 (1.0–1.5)

[a] At 22 °C, pH 7.50, corrected to zero ionic strength; 10% (v/v) ethanol. Values in parentheses for Sr^{2+} and Ba^{2+} indicate ranges which give nearly equivalent fits. Errors are (parameter variance)$^{1/2}$; spectra reproduce with a standard deviation of 0.3–0.5%. [b] $[H^+] = 3.16 \times 10^{-8}$ M at pH 7.50.

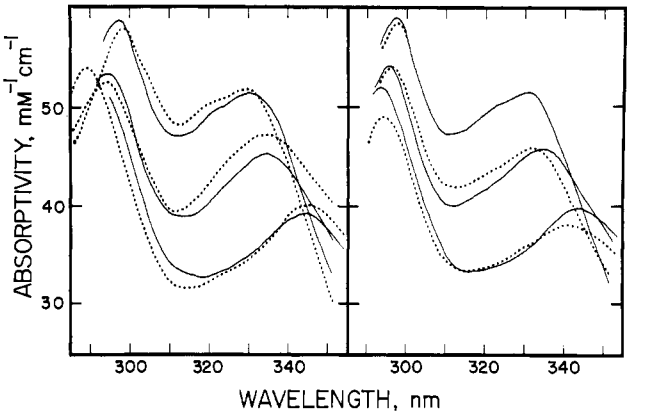

FIGURE 2: Spectra of thermorubin–M^{2+} complexes. Spectra computed from 10–15 data sets each: see also Table I. Left, Mg^{2+} (···), Ca^{2+} (—); right, Sr^{2+} (—), Ba^{2+} (···). Reading down at 320 nm, one observes the following species: mixed $TrH_n^{(3-n)-}$ at pH 7.5 (mostly TrH^{2-}); TrH·M; $Tr{\cdot}M_2^+$. The three curves for Ca^{2+} and Sr^{2+} solutions are almost identical.

Terms in brackets are activities: $[X_i] \equiv (X_i)f_i$. The f_i values are obtained from the extended Debye–Hückel expression adequate for ionic strengths μ below 0.05 M: $\log f_i = -AZ_i^2\mu^{1/2}/(1 + B\mu^{1/2})$, with A evaluated for 10% ethanol at 22 °C; the size parameter B was taken as 1 for the smaller cations and buffer ions and as 2 for the larger thermorubin species.

A priori, it cannot be decided whether $Tr{\cdot}Mg^-$ is a significant species at pH 7.50 or whether loss of the third proton occurs mainly via eq 3.4. However, since the ratio of concentrations $(Tr{\cdot}Mg^-)/(TrH{\cdot}Mg)$ is almost invariant at fixed pH and nearly constant μ (eq 3.2), an a priori decision is not required. The actual fittings for a given pH series can use the mixed species ML′, where (ML′) = (TrH·Mg) + ($Tr{\cdot}Mg^-$) and the parameters L'_{11} and L'_{12} are defined

$$L'_{11} \equiv (ML')/([TrH^{2-}][Mg^{2+}]) = L_{11}\{1 + K_{3M}/([H^+]f_{-1})\} \qquad (3.5)$$

$$L'_{12} \equiv [TrMg_2^{2+}]/\{(ML')f_{-1}[Mg^{2+}]\} = L_{12}/\{1 + f_{-1}[H^+]/K_{3M}\} \qquad (3.6)$$

The values obtained for L'_{11} and L'_{12} for Mg^{2+}, Ca^{2+}, Sr^{2+}, and Ba^{2+}, at pH 7.50, are listed in Table I. Obviously, the larger Sr^{2+} and Ba^{2+} cations strain the "bite" of thermorubin, which is adapted for its natural M^{2+}, Mg^{2+}.

The derived spectra of ML′ and M_2L are shown in Figure 2. The spectra for ML′ strongly resemble the spectrum of TrH^{2-}, clearly implying that TrH·M predominates over $Tr{\cdot}M^-$, that K_{3M} is not much larger than K_3, and that the main pathway to M_2L^+ is via eq 3.4. The fittings with L_{11} and L_{12H} naturally give similar results (Table I). The spectra of M_2L likewise resemble that of Tr^{3-}, confirming that M_2L is $Tr{\cdot}M_2^+$.

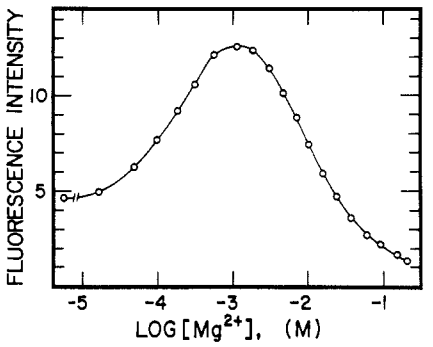

FIGURE 3: Mg^{2+} concentration dependence of thermorubin fluorescence. Thermorubin (2.0×10^{-6} M) in standard buffer, no Mg^{2+} (treated with Chelex-100), was titrated with 2 M $Mg(OAc)_2$ in the same buffer, 25 °C. Emission, 590 nm; excitation, 334 nm.

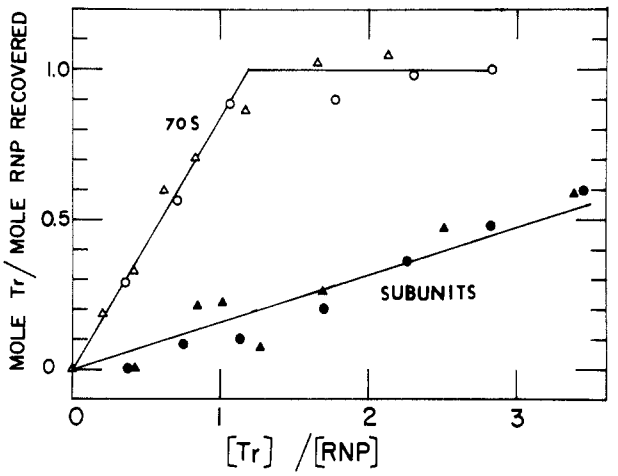

FIGURE 4: Stoichiometry of thermorubin binding by preparative ultracentrifuation. Thermorubin recovery was determined by absorption spectrophotometry at 340 nm, corrected for ribosomal particle turibidity as described in the text. Ordinate, moles of thermorubin bound per mole of ribosomal particle in the washed, resuspended pellet. Abscissa, ratio of thermorubin to ribosomal particle concentration in the original solution before centrifugation (10 mM Mg^{2+} standard buffer, 2% v/v Me_2SO, 4 °C). (○) 2.81×10^{-7} M 70S ribosomes, SW 41 rotor; (△) 1.21×10^{-7} M 70S ribosomes, Ti 60 rotor; (●) 2.14×10^{-7} M 30S subunits, Ti 60 rotor; (▲) 1.18×10^{-7} M 50S subunits, Ti 60 rotor.

These conclusions are reinforced by the results with Mg^{2+} at pH 6.0: with the fraction of TrH^{2-} cut from 0.75 to 0.09, L'_{11} is still $(3.7 \pm 0.4) \times 10^4$ M^{-1}, while L'_{12} is about 20 M^{-1}, compared to 3.3×10^4 and 400 M^{-1} at pH 7.50. K_{3M} is clearly small (cf. eq 3.5 and 3.6).

The sequential formation of TrH·Mg and $Tr{\cdot}Mg_2^+$ may also be observed in fluorescence studies (Figure 3). The curve is in excellent agreement with the predictions from L'_{11} and L'_{12} at this pH and ionic strength. The intensity falls off at high $[Mg^{2+}]$ because $Tr{\cdot}Mg_2^+$ is not fluorescent, not because of any quenching phenomenon: the excitation spectra do not follow the observed absorbance shifts (cf. Figure 2) but simply reflect the progressive decrease in [TrH·Mg].

(B) Thermorubin Binding to Ribosomal Particles. Ultracentrifuge Studies. Figure 4 shows the 4 °C equilibrium binding curves for the ribosome and its subunits. The principal conclusion to be drawn from this result is perfectly clear and unambiguous: there is a strong stoichiometric 1:1 binding of thermorubin to the 70S particle. Binding to 30S or 50S subunits is much weaker: the association constants are at least 1 order of magnitude smaller. Weak binding to 70S particles, if any, is insignificant compared to the strong binding in this range, although one might have drawn slightly sloping lines through the data above the equivalence point. Studies using a fluorescence assay for thermorubin recovery yield identical conclusions (data not shown).

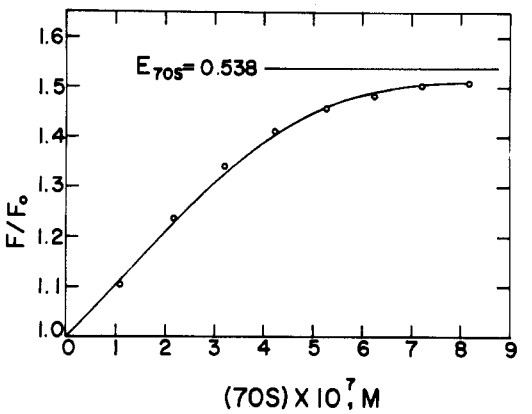

FIGURE 5: Fluorescence enhancement titration of thermorubin with ribosomes. Thermorubin, 5×10^{-7} M, was in 10 mM Mg^{2+} standard buffer, 2% v/v Me_2SO, filtered, at 25 °C, and increments of 70S ribosomes were present as indicated. Ordinate, ratio of corrected fluorescence intensity F to the value F_0 in the absence of ribosomes. Circles, experimental results; solid curve, computer fit yielding $K_D = 1.9 \times 10^{-8}$ M, $E = 0.54$.

Fluorescence Enhancement Determinations of Thermorubin Binding. The addition of ribosomes or subunits to a thermorubin solution produces an increase in the fluorescence intensity, which can be used for a convenient and accurate determination of the number of binding sites and their dissociation constants. We define F and F_0 as the fluorescence intensities in the presence and absence of ribosomal particles; $(F - F_0)/F_0 = E$ is the enhancement, and its limiting value at infinite ribosomal particle concentration is the limiting or specific enhancement, E_∞.

Two approaches were used: the first tends to select for high-affinity sites, since the thermorubin concentration is always very low; the second sacrifices precision at the high-affinity end for indications of weaker binding.

Titration with Ribosomes at a Fixed Concentration of Thermorubin. A 70S ribosome titration curve is shown in Figure 5. The tight binding of thermorubin is indicated by the steep rise in F/F_0 at low ribosome concentrations and the rapid appearance of a plateau after 1 equiv of ribosomes has been added. The only model which can successfully fit this isotherm is the simplest: a single binding site on the ribosome, with dissociation constant $K_D = 1.9 \times 10^{-8}$ and $E_\infty = 0.54$.

70S particles bind thermorubin with *very* high affinity: binding of streptomycin is at least 5 times weaker (Hall et al., 1977); binding of chloramphenicol or tetracyclines is orders of magnitude weaker (Weissbach & Pestka, 1977; Fey et al., 1973).

The curves for addition of 30S and 50S subunits are shown in Figure 6. Fitting for a single site on each subunit gave values of 1.41 and 1.53 for the limiting enhancement and 1.9×10^{-6} and 1.4×10^{-6} M for K_D, for the 30S and 50S subunits, respectively. These dissociation constants are at least 100 times weaker than the K_D for 70S particles (the values also show that contamination of the 70S sample with small amounts of 50S particles will have negligible effects). The experimental design, ribosomal particle excess, as noted, tends to focus primarily on the binding site with the highest affinity.

Titration with Antibiotic at a Fixed Concentration of Ribosomes. The nearly quantitative binding to the strong site, in ribosome excess, is indicated in the F/F_0 plateau at 1.53 (Figure 7); recall that E_∞ is 0.54. The existence of additional, weaker, binding is indicated by the shape of the F/F_0 curve

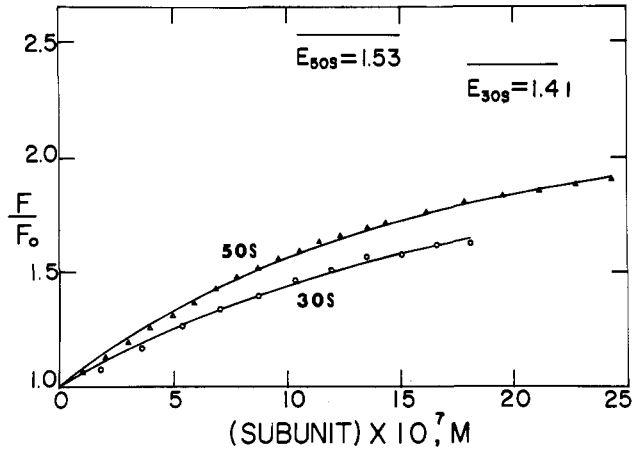

FIGURE 6: Fluorescence enhancement titration of thermorubin with ribosomal subunits. Conditions as described in Figure 6, except that the titrants were concentrated subunit solutions. 30S subunits: (O) experimental points; (—) computer fit yielding $K_D = 1.9 \times 10^{-6}$ M, $E = 1.41$. 50S subunits: (Δ) experimental points; (—) curve for $K_D = 1.4 \times 10^{-6}$ M, $E = 1.53$.

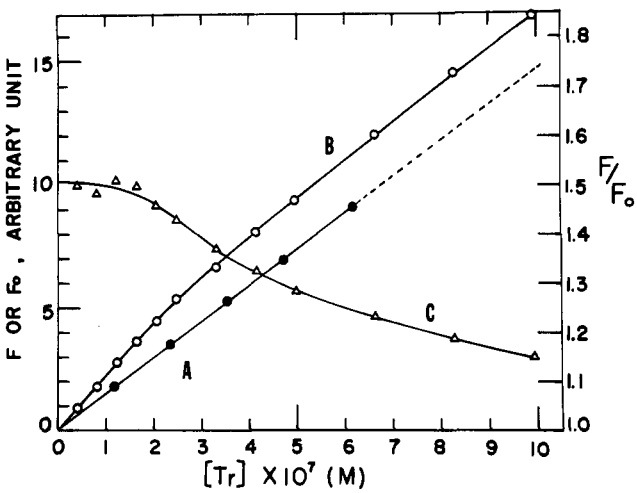

FIGURE 7: Fluorescence enhancement study of thermorubin binding to 70S ribosomes by antibiotic titration. Prefiltered 10 mM Mg^{2+} standard buffer (40–50 mL) (2% Me_2SO v/v), in the presence or absence of 70S ribosomes, was titrated with aliquots of 1 mM thermorubin solution in Me_2SO. Thus, the final level of Me_2SO increases only to 2.5–3.0% v/v. (A, ●) Thermorubin fluorescence, F_0, in the absence of ribosomes; (B, O) thermorubin fluorescence, F, in the presence of 1.3×10^{-7} M 70S ribosomes (left ordinate); (C, Δ) fluorescence ratio, F/F_0 (right ordinate).

and the nonparallelism of the upper A and B lines: at a Tr/70S ratio of 8, the enhancement, 0.15, is double the value expected for the strong site alone, 0.07. This moderate increment is best explained as fractional double occupancy of the strong site (see below) with the 3-fold larger E_∞ characteristic of subunits; binding to the few percent of contaminating 50S subunits contributes 15–20% of the difference. There is no sign of the bizarre multiple binding reported for tetracyclines (Fey et al., 1973).

A word must be said about the magnitude of the E_∞ values. In the case of 70S complexes, the enhancement could be argued to arise from a shift in the $TrH{\cdot}Mg/TrMg_2^+$ ratio as a result of binding of the fluorescent $TrH{\cdot}Mg$ species to the ribosome (cf. Figure 3). The larger E_∞ values for the 30S and 50S subunits certainly imply some additional specific effect of binding. Speculation on the origin of this effect would be premature.

It might be argued that the subunits give the same limiting enhancement as the 70S particles but have only fractional populations capable of binding thermorubin. If, for example,

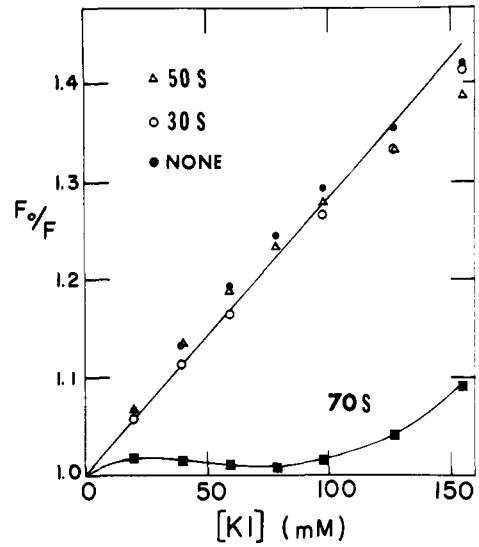

FIGURE 8: Iodide ion quenching of thermorubin fluorescence. Thermorubin, 5×10^{-7} M, in 10 mM Mg^{2+} standard buffer at 25 °C (2% Me_2SO v/v) was titrated with 5 M KI (in the presence of 10^{-4} M $Na_2S_2O_3$ to prevent I_3^- formation) in the presence or absence of ribosomal particles. Note that in this series F_0 is the total fluorescence intensity, *including* emission from thermorubin bound to ribosomal particles, at zero *iodide* concentration; F is the intensity of that solution at the given $[I^-]$. (●) No ribosomal particles; (O) 1.37×10^{-6} M 30S subunits; (Δ) 8.8×10^{-7} M 50S subunits; (■) 5.0×10^{-7} M 70S ribosomes.

the 30S–50S protein S20 = L26 were involved in the binding site, roughly half of each subunit preparation might retain the capacity for binding the antibiotic. This hypothesis is not really tenable. The fits not only are poorer but also are systematically poorer: the hypothesis distorts the *shape* of the isotherms.

Iodide Quenching Studies. The binding sites were further characterized by studies of quenching by iodide ion. For simple Stern–Volmer collisional quenching, the observed intensity F should decrease as $F_0/F = 1 + KQ$, where Q is the concentration of quencher and K is the product of a second-order quenching constant and the excited-state lifetime. Note that here F_0 is the intensity in the absence of quencher and includes enhancements due to binding by ribosomal particles. Thermorubin bound to 30S or 50S subunits is quenched as efficiently as free thermorubin: curves with the same K are obtained under conditions where a substantial fraction of thermorubin is bound (39% and 33% for 30S and 50S subunits, respectively) (Figure 8). Significant differences in quenching would have been easy to see. The subunit sites are therefore freely accessible to I^-. In contrast, thermorubin bound to 70S particles is virtually unquenchable. It is, therefore, inaccessible to I^- (by 0.15 M KI, some dissociation of 70S particles would have occurred).

A highly attractive hypothesis, obviously not yet firmly established, is that the 30S and 50S sites are located at the 30S–50S interface and that each binds only a portion of the molecule; the uniquel 70S site which binds the entire thermorubin molecule would be formed by the union of the partial sites. In this context, the apparent weak site on 70S particles implied by Figure 7 would be ascribed to the binding of two molecules of thermorubin separately in the 30S and 50S components of the 70S strong site; such effects are seen in cases of substrate inhibition of enzymes, where the existence of multiple points of interaction on the substrate results in weaker, sterile, double occupancy of the active site at higher concentrations. On the other hand, the K_D of dissociation of 70S thermorubin complexes is much larger than the product $K_{D,30S}K_{D,50S}$, so the separate free energies are not additive;

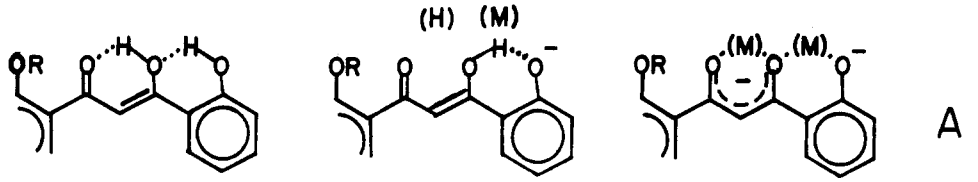

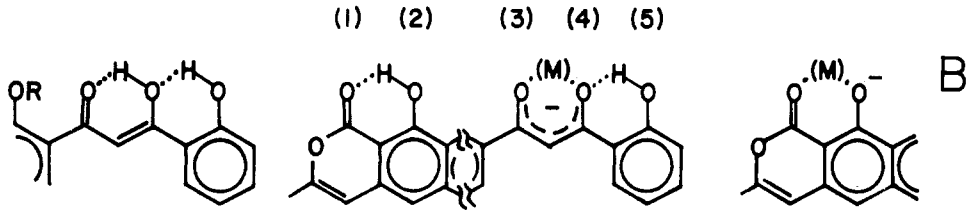

$$TrH_2^- = TrH^{2-}(TrH{\cdot}Mg) = Tr^{3-}(Tr{\cdot}Mg_2^+)$$
$$+ H^+ \qquad + 2H^+$$

again, in this context, formation of the empty 70S site is a free-energy-requiring process, relieved by the negative free energy of filling the site with thermorubin. In other words, the equilibrium conformation of a vacant 70S particle is different energetically, and so in some sense structurally, from the 70S conformation in the thermorubin complex. It raises the possibility that one of the stages leading to the formation of the initiation complex (initiator tRNA·mRNA·70 S) has a configuration more conducive to binding of thermorubin and can be trapped or decomposed into a form that would not score as initiator binding in the filter-binding assay.

Effects on the Association of Subunits. Finally, the stronger binding of thermorubin to 70S particles implies a corresponding rightward shift in the $[Mg^{2+}]$-dependent 30S + 50S $\rightleftharpoons$ 70S equilibrium, which can be confirmed by light scattering or sedimentation studies. For example, in sucrose density gradient analyses of glutaraldehyde-fixed samples, it could be seen that addition of thermorubin had increased the fraction of 70S particles from 0.14 to 0.39 at 1 mM Mg^{2+} and from 0.63 to 0.78 at 2 mM Mg^{2+}. By 5 mM Mg^{2+}, 70S formation in this type A preparation is nearly complete in either case.

Note that the concentration of thermorubin at which significant effects are observed, 2.5×10^{-7} M in this case, is 2–4 orders of magnitude smaller than that for polycationic effects which are reported to promote 70S formation [e.g., polyamines, approximately millimolar; for the aminoglycosides neomycin, 2×10^{-5} M, streptomycin, 2×10^{-4} M, and dihydrostreptomycin, 2×10^{-3} M (Leon & Brock, 1967)]. A major component of the latter effect, multiple binding and concomitant decrease of the negative charge on the ribosomal particles, is clearly not significant for 1:1 thermorubin–ribosome complexes; the effect is obviously quite specific.

(C) Thermorubin H^+–M^{2+} Equilibria. The structural consequences of this work are (a) that the published structure (I) with phenols and a hydroxyxanthone, which has no, let alone two, groups with a pK_a below 9–10 [cf. Saxena & Sheshadri (1957)], is completely incompatible with our results and (b) that the newly proposed structure (II) (Johnson et al., 1980) is compatible, given a certain amount of handwaving.

The first pK_a of 4.7 is of course that of the aliphatic carboxylic acid. However, large spectral shifts are not expected for ionization of an unconjugated COOH (cf. Figure 1). Presumably, the charge and/or hydrogen-bonding properties of the COO^- or COOH, or their indirect effects on the local water structure, shift the equilibrium among the several tautomeric keto–enol forms and the diketone [the equilibrium constants in water are not likely to be more than an order of magnitude from unity [cf. Battesti et al. (1974) and references cited therein]]. In organic solvents, 1,3-diphenyl-1,3-propanediones will be present 100% as the strongly internally chelated keto–enols [cf., e.g., Battesti et al. (1974)]; in thermorubin crystallized from $CHCl_3$, it is O_4 which is enolized (Johnson et al., 1980). The spectrum of TrH_2^-, at pH 6, is the one which resembles the spectra of thermorubin in $CHCl_3$, dimethylsulfoxide (Me_2SO), and ethanol showing in particular the rippling sequence of peaks at 302, 316, and 330 nm with intensities around 50000 $cm^2\ M^{-1}$ (301, 315, and a slightly more prominent 330 nm in $CHCl_3$). The TrH_2^- spectrum increasingly predominates as the ethanol concentration is increased: the dramatic decrease in absorbance between pH 6 and 2 in 10% ethanol is replaced by a much smaller decrease in 20% ethanol, which almost disappears in 50% ethanol. One concludes that in water the TrH_3 species has one predominant tautomer, perhaps the diketone; the TrH_2^- species is largely enolic, with quite possibly the O_3(oxo)–O_4(hydroxy) structure observed in the crystal.

A definitive assignment of the remaining sites of successive proton dissociation and cation binding cannot be made at this time. However, one can discuss two plausible sequences, A and B.

Johnson et al. (1980) interpreted our H^+ equilibria in terms of sequence A ($COOH > O_5 > O_4 \gg O_2$) essentially because NMR and degradation studies of the trimethyl derivative of thermorubin indicated that O_4 and O_5, but not O_2, were able to react with diazomethane. A low pK_a for the O_5 phenol can be justified from the hydroxybenzaldehyde and hydroxyacetophenone values (Sillén & Martell, 1971), and the $Tr{\cdot}Mg_2^{2+}$ structure we would assign in the A sequence may be compared to the M_2L_2 complexes of 1,3,5-triketones formed in nonpolar media (Glick & Lintvedt, 1976): the O_3–O_4–O_5 oxygen atoms do line up this way in the TrH_3 crystal (Johnson et al., 1980). However, this sequence has difficulties with the nonequivalence of TrH^{2-} and TrH·Mg, and the corresponding structures do not seem to justify high values for pK_4 in Tr^{3-} or for pK_{3M} in TrH·Mg or the relatively low pK_3 in TrH^{2-} (see below). Moreover, an –OH similar to O_2, in a 1-hydroxy-

xanthone, can be methylated (Johnson et al., 1980), while treatment of the model compound 1-(2-hydroxyphenyl)-3-phenyl-1,3-propanedione with diazomethane reportedly yielded only the monomethylated (2-methoxyphenyl) derivative (Dewar & Sutherland, 1977).

We prefer sequence B largely because the keto–enol of TrH_2^- is the exact electronic and geometric "vinylogue" of salicylic acid. In salicylic acid, the pK_a of the carboxyl group (the vinylogue of the O_3–O_4 keto–enol) is anomalously low (2.97, compared to 4.5 for 4-hydroxybenzoic acid), and the phenolic pK_a is extraordinarily high (13.59, compared to 9.3 for 4-hydroxybenzoic acid; Sillén & Martell, 1964) because the intermediate monoanion is stabilized by a spectacularly tenacious hydrogen bond. Similar stabilization of hydroxy–oxy anion intermediates is observed in malonic acids (Tanford, 1957). We still have to handwave a reduction in pK_2 by interactions from the fused-ring moiety of thermorubin, since the pK_1 of 1-(2-hydroxyphenyl)-3-phenyl-1,3-propanedione in water is 8.8 (Pelizzetti & Verdi, 1973). However, both Pelizzetti and Verdi and Fernelius and co-workers [references passim in Sillén & Martell (1964)] assign the observable pK_a in the latter and related compounds to the keto–enol rather than the 2-hydroxyphenyl portion of the molecule.

Supplementary Material Available

Appendix I containing three criteria for acceptance of the ML–M_2L sequence and Figure A1 showing the stoichiometry of Mg^{2+}–thermorubin complexes (3 pages). Ordering information is given on any current masthead page.

References

Battesti, P., Battesti, O., & Sêlim, M. (1974) *Bull. Soc. Chim. Fr.*, 2214–2220.

Craveri, R., Coronelli, C., Pogani, H., & Sensi, P. (1964) *Clin. Med. 71*, 511–521.

Dewar, D. J., & Sutherland, R. G. (1977) *J. Chem. Soc., Perkin Trans. 2*, 1522–1526.

Fey, G., Reiss, M., & Karsten, H. (1973) *Biochemistry 12*, 1160–1164.

Glick, M. D., & Lintvedt, R. L. (1976) *Prog. Inorg. Chem. 21*, 233–260.

Hall, J., Davis, J. P., & Cantor, C. R. (1977) *Arch. Biochem. Biophys. 179*, 121–130.

Johnson, F., Chandra, B., Iden, C. R., Naiksatam, P., Kahen, R., Okaya, Y., & Lin, S.-Y. (1980) *J. Am. Chem Soc. 102*, 5580–5585.

Leon, S. A., & Brock, T. D. (1967) *J. Mol. Biol. 24*, 391–404.

Lin, F. (1978) Ph.D. Thesis, State University of New York at Stony Brook.

Lin, F., & Wishnia, A. (1982) *Biochemistry* (following paper in this issue).

Moppett, E., Dix, D. T., Johnson, F., & Coronelli, C. (1972) *J. Am. Chem. Soc. 94*, 3269–3272.

Nancollas, G. H. (1956) *J. Chem. Soc.*, 744–749.

Pelizzetti, E., & Verdi, C. (1973) *J. Chem. Soc., Perkin Trans. 2*, 808–811.

Pirali, G., Somma, S., Lancini, G. C., & Sala, F. (1974) *Biochim. Biophys. Acta 366*, 310–318.

Saxena, G. M., & Sheshadri, T. R. (1957) *Proc.—Indian Acad. Sci., Sect. A 46A*, 218–223.

Sillén, L. G., & Martell, A. E. (1964) *Stability Constants of Metal-Ion Complexes*, Suppl. 1, Spec. Publ. No. 17, The Chemical Society, London.

Sillén, L. G., & Martell, A. E. (1971) *Stability Constants of Metal-Ion Complexes*, Suppl. 1, Spec. Publ. No. 25, The Chemical Society, London.

Stone, W. L., & Wishnia, A. (1978) *Bioinorg. Chem. 8*, 517–529.

Tanford, C. (1957) *J. Am. Chem. Soc. 79*, 5348–5352.

Tritton, T. R. (1977) *Biochemistry 16*, 4133–4138.

Weissbach, H., & Pestka, S., Eds. (1977) *Molecular Mechanisms of Protein Biosynthesis*, Academic Press, New York.

White, J. P., & Cantor, C. R. (1971) *J. Mol. Biol. 58*, 397–400.

Wishnia, A., & Boussert, A. (1977) *J. Mol. Biol. 116*, 577–591.

Wishnia, A., Boussert, A., Graffe, M., Dessen, Ph., & Grunberg-Manago, M. (1975) *J. Mol. Biol. 93*, 499–515.